Arch. Metall. Mater. **68** (2023), 3, 1121-1126

DOI: https://doi.org/10.24425/amm.2023.145483

P. CZAJA[1*]

LORENTZ TEM AND LM-STEM DPC ANALYSIS OF MAGNETIC DOMAINS IN SOFT FERROMAGNETS

Magnetic microstructure in the as suction cast $Fe_{69}B_{20}Nb_2Hf_2Si_2Y_5$ alloy was revealed by combined Lorentz-TEM and LM-STEM DPC analysis. The thin foil of the alloy was found to be composed primarily of the amorphous phase with few dendritic structures. Magnetic domains were found large in the μm range with an average domain wall width of 52 nm. The magnetic domain boundaries are easily mobile, what was confirmed by in situ applied magnetic field. The LM-STEM DPC complements the Lorentz-TEM analysis by providing details on the intensity and spatial distribution of the magnetization vector within the domains.

Keywords: Lorentz-TEM; STEM-DPC; magnetization; magnetic domains; soft ferromagnets

1. Introduction

It is a fascinating historical recollection that the domain theory, originally introduced by Weiss in 1906, was long left more widely unrecognised and even Weiss himself put more emphasis to molecular field theory rather than domain theory. It was not until forty three years later when first experimental evidence emerged to corroborate the domain structure of a real material and to make the domain theory fully blossom. Since that time the domain theory has become foundational to explaining the intricacies of magnetisation process and it largely has shaped our understanding of magnetic behaviour of materials [1].

Along with the advances on the more theoretical front much progress was made over the ensuing years in magnetic domain imaging. Visualization of magnetic domains, assessing their spatial distribution, size, shape and arrangement greatly complements theoretical modelling and thermomagnetic measurements and is thus indispensable for accurate characterization of magnetic materials. For observation a range of methods were devised. In principle all those methods can be grouped into two classes: (*i*) these that disclose the domain walls (Bitter method, scanning probe microscope, Lorentz Microscopy in Fresnel mode) and the second class (*ii*) permitting observation of domains themselves through contrast or colour changes (Kerr, Faraday effects, polarized electron analysis, holography, differential phase contrast). Likewise on the instrumental side, given the mesoscopic size of typical domains, the frequently employed microscopy techniques can be subdivided into light and electron microscopy [1].

Among the latter transmission electron microscopy (TEM) has the most appeal given its high spatial resolution capabilities and additional information on chemical composition and local structure it can yield simultaneously while examining magnetic thin foils. It also allows for real time experiments with in-situ applied magnetic field or temperature, what provides much desired means for studies of the dynamics of magnetic domains. The foremost limitation in this instance is the thin foil thickness, which has to be thin enough to be transparent for electron beam [2].

The physical principles of TEM domain imaging require that there is no magnetic field in the sample area into which, if present, the thin lamella would be otherwise immersed with fatal effect for the original domain structure. There is a number of technical strategies to ensure a magnetic free zone and the most common approach is simply realised by switching off the objective lens. Once this condition is met and the beam is directed vertically towards the thin foil it suffers a deflection force, Lorentz force, exerted by the ferromagnetic component lying in a plane perpendicular to the electron trajectory. The magnitude of the Lorentz force is proportional to the vector product of electron velocity ($\boldsymbol{v}$) and magnetic induction ($\boldsymbol{B}$) averaged along the electron path: $\boldsymbol{F} = |e|(\boldsymbol{v} \times \boldsymbol{B})$ Hence the operating TEM

[1] THE ALEKSANDER KRUPKOWSKI INSTITUTE OF METALLURGY AND MATERIALS SCIENCE POLISH ACADEMY OF SCIENCES, 25 REYMONTA STR., 30-059 KRAKÓW, POLAND

* Corresponding author: p.czaja@imim.pl

mode is named Lorentz TEM. The Lorentz deflection angle β_L is given by

$$\beta_L = \frac{e\lambda t}{h} \boldsymbol{B}_\perp$$

where λ is the relativistic electron wavelength, t stands for the local sample thickness, h is Planck's constant and $\boldsymbol{B}_\perp$ is the magnetic induction component normal to the electron trajectory. Typical Lorentz angle is below 100 μrad what is not trivial since it averts the risk of confusing Lorentz deflection angle with the more common Bragg scattering angle occurring typically in the 1-10 mrad range [2].

The most commonly exploited Lorentz TEM mode is the Fresnel mode. Depending on the defocus conditions (under focus, in focus, over focus) the magnetic domains are imaged as alternate bright and dark lines, the contrast is reversible when going from under to over focus *i.e.* bright lines become dark, dark turn into bright and so on. The mechanism of contrast generation is based on the domain walls arrangement relative to the electron beam. The bright lines turn up if the domain walls are arranged in such a way that the beam on either side of the wall is deflected towards the wall (convergent). When examined more closely bright lines, in fact, are composed of a set of parallel fringes, whose interpretation is quite complex and at the first approximation they can be understood in terms of local magnetic field fluctuations or field gradient in close proximity to the wall. The dark lines, as can be logically deduced, result from such a wall arrangement, that on either side of the wall the beam is deflected away from the wall. Although very useful for fast domain wall analysis and permitting real time in-situ studies on *e.g.* magnetization reversal Lorentz TEM fails short when it comes to spatial distribution analysis of magnetization vector and it's intensity within the domain area.

In this respect more informative is differential phase contrast (DPC) analysis realised in scanning transmission electron microscopy (STEM) mode [3,4]. In simple terms in STEM a fine probe is scanned over a sample surface and at each raster electrons that are transmitted and scattered fall on a donut shaped, annular detector (ADF) placed beneath the sample. The resulting image contrast is roughly proportional to the square of the atomic number and hence the mode is particularly suited to heavy elements. Owing to the recent advances in aberration correction technology it allows for direct observation of columns of atoms and individual atoms what in conjunction with energy dispersive spectroscopy (EDS) makes it particularly attractive for research fields requiring precise atomic structure identification. On top of the atomic structure analysis STEM can be used to map electro-magnetic fields. Successful mapping requires a separate split detector capturing a transmission disk at each scanning point. Owing to the same Lorentz force acting on the electron trajectory the beam is deflected and the deflection is measured as differential between the opposing segments of split, quadrant detector, employed to capture the transmitted disk after passing through the sample.

In what comes next I discuss the application of Lorentz TEM and LM-STEM DPC to evaluation of magnetic microstructure in an example suction cast $Fe_{69}B_{20}Nb_2Hf_2Si_2Y_5$ soft ferromagnetic alloy [5].

2. Experimental

The specimen under investigation was produced from a master ingot by suction casting. The nominal chemical composition of the specimen was $Fe_{69}B_{20}Nb_2Hf_2Si_2Y_5$ (at.%) and it was consistent with the measured EDS composition, which was $Fe_{88.4}Nb_{1.9}Hf_{2.7}Si_{2.2}Y_{4.8}$ (at.%). Thin lamellae for TEM were cut with focused ion beam (FIB) technique employing Thermo-Scientific Titan Themis X-FEG G3 Cs-corrected S/TEM microscope. More details can be found elsewhere [6].

3. Results and discussion

The Fig. 1 shows a high resolution (HRTEM) image (a) and the corresponding Fast Fourier Transform (FFT) pattern taken (b) from the thin lamellae of the as suction cast $Fe_{69}B_{20}Nb_2Hf_2Si_2Y_5$ alloy. The HRTEM micrograph (Fig. 1a) is typical for an

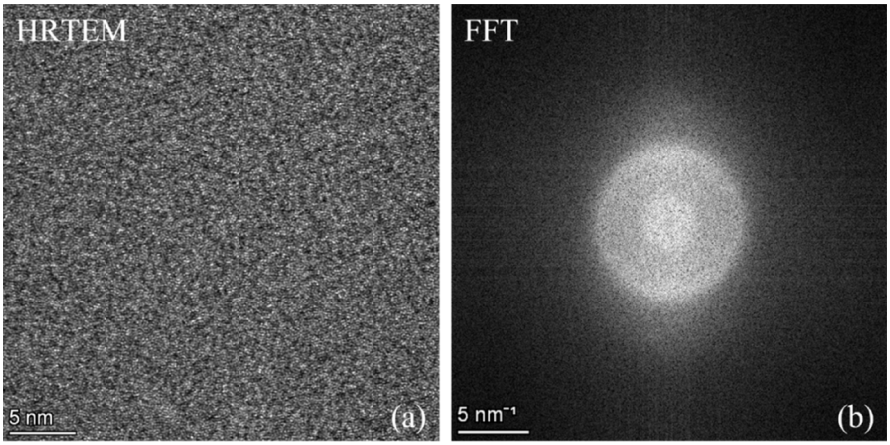

Fig. 1. The high resolution TEM (HRTEM) image (a) and the corresponding Fast Fourier Transform (FFT) (b) pattern taken from the thin lamella of the $Fe_{69}B_{20}Nb_2Hf_2Si_2Y_5$ as suction cast alloy

amorphous material and the corresponding FFT shows in accordance a diffuse pattern (Fig. 1b). This well is in agreement with X-ray diffraction studies (not shown).

The Fig. 2 shows Lorentz TEM images taken at the same magnification from the thin lamella of the $Fe_{69}B_{20}Nb_2Hf_2Si_2Y_5$ alloy at different values of defocus: 947 μm (a), 35 μm (b) and –976 μm (c). The top layer of the lamella with dark contrast than rest of the specimen is made of Pt used for screening against Ga^+ ions, while FIB etching. Beneath the Pt top layer the thin lamellae does not display any microstructural features apart from the dendrite structures, clearly visible on the in focus image in the Fig. 2b. The dendrites appear in response to suction casting, which kinetically and thermodynamically differs from melt spinning that is more widely used for fabrication of soft ferromagnets. Irrespective of the dendritic structures Lorentz TEM reveals the presence of distinct magnetic domain boundaries, which disappear under in-focus conditions (Fig. 2b) and reappear under out of focus conditions (Fig. 2a,c). The domains are large in μm range and the domain boundary contrast changes from dark to bright, when switching from over focus (Fig. 2a) to under focus (Fig. 2c).

For a more detailed inspection of a magnetic domain wall structure a series of images were taken at different values of under focus (Fig. 3a-d). At the –2.3 mm under focus (Fig. 3a) the domain wall boundary is composed of a number of parallel fringes. The number of fringes decreases as the focus parameter approaches in focus conditions (Fig. 3b-d). The exact origin of these fringes is quite complex for interpretation but at the first approximation it can be related to the magnetic field gradient in close proximity to the domain wall as was already discussed in the introduction.

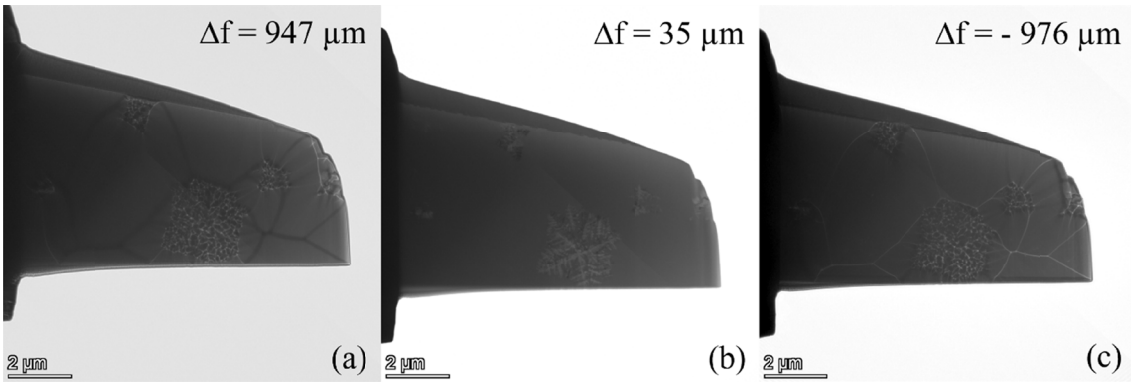

Fig. 2. Lorentz-TEM micrographs taken at different focus from the thin lamella of the $Fe_{69}B_{20}Nb_2Hf_2Si_2Y_5$ alloy

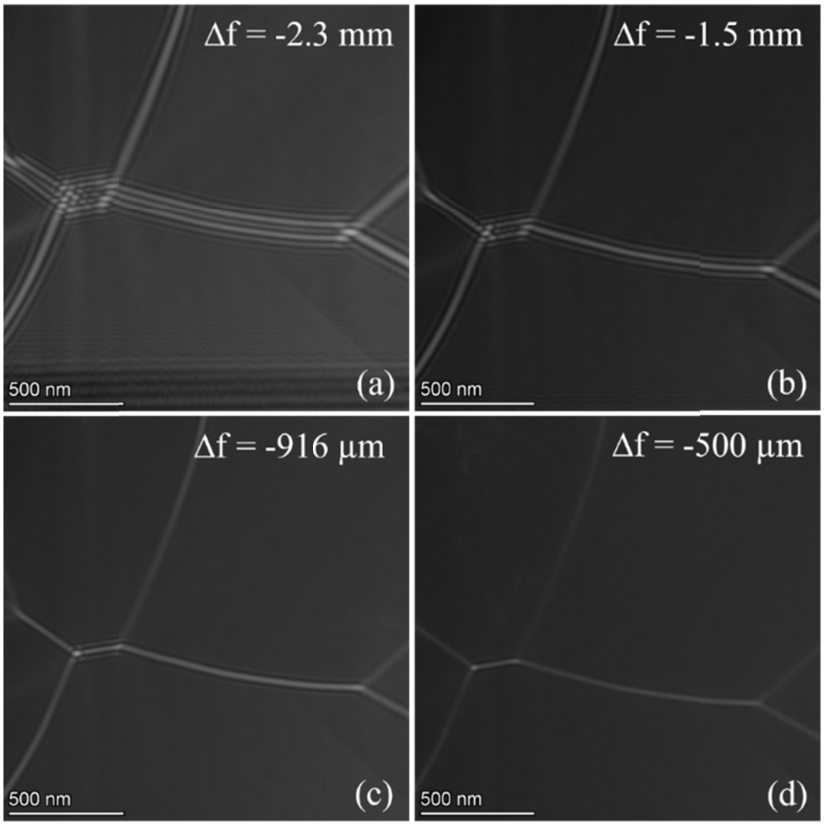

Fig. 3. A series of TEM Lorentz taken for the thin lamella of the $Fe_{69}B_{20}Nb_2Hf_2Si_2Y_5$ alloy at different values of under focus

An average width of the domain wall boundary can be determined by taking a series of out of focus images, with varying focus, and then plotting the image estimated domain wall width as a function of defocus parameter [7]. An example image taken from the current specimen at 1.6 mm over focus is shown for illustration in the Fig. 4(a). The green marker on the image indicates the observed domain wall width at that over focus value. The measured domain wall width as a function of defocus parameter is plotted in the Fig. 4 (b). By simple extrapolation to zero defocus it was possible to estimate the average domain wall width in the current specimen at 52 nm.

For analysis of the domain boundary mobility magnetic field was applied in situ by running the electric current through the objective lens. The applied current value was restricted to 10% of nominal value. For illustration most exemplary images taken at 0%, 5% and 10% current are presented at the Fig. 5(a-c). From the images it can be easily spotted that as the intensity of the current applied increases the domain walls shift and at the same time larger domains grow in size at the expanse of the smaller ones. It can be also noticed that the dendritic structures, although showing magnetic microstructure themselves, act as pinning sites for the walls of large domains.

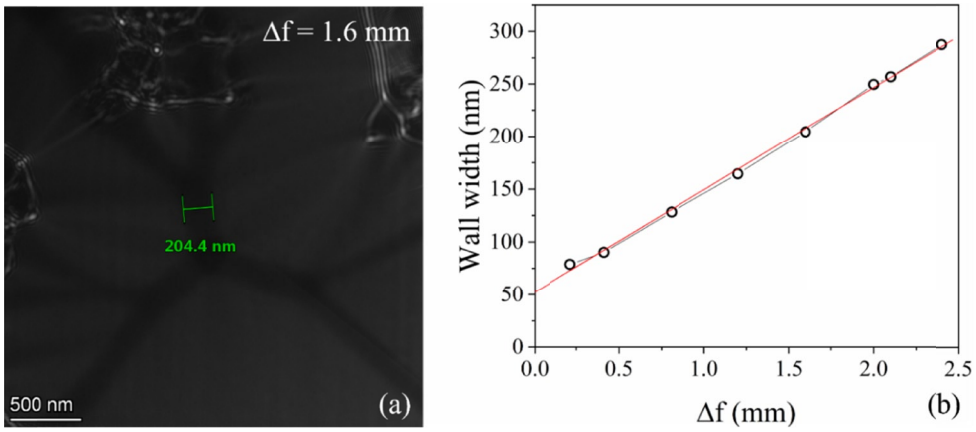

Fig. 4. Lorentz TEM micrograph taken at 1.6 mm over focus with a measured and marked domain wall width (a). The domain wall width a as function of defocus (Δf) plotted based on a series of over focus Lorentz-TEM images (b)

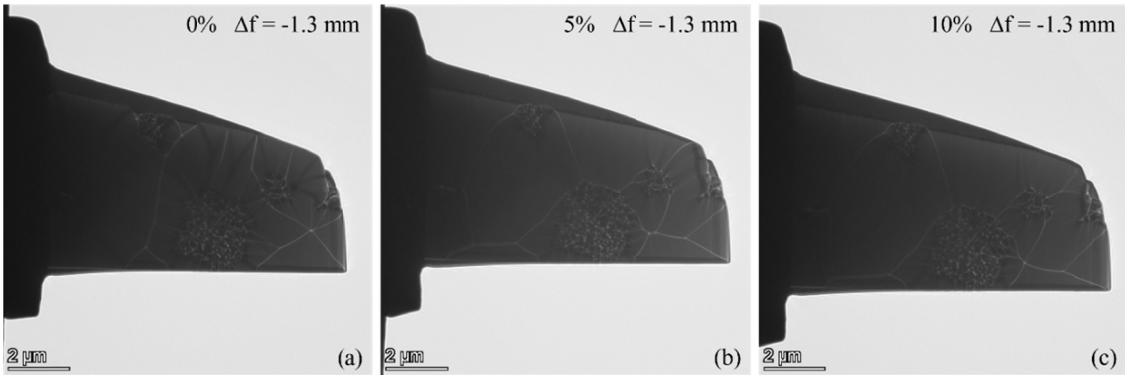

Fig. 5. A sequence of Lorentz-TEM images taken at the same under focus (-1.3 mm) under in situ applied magnetic field

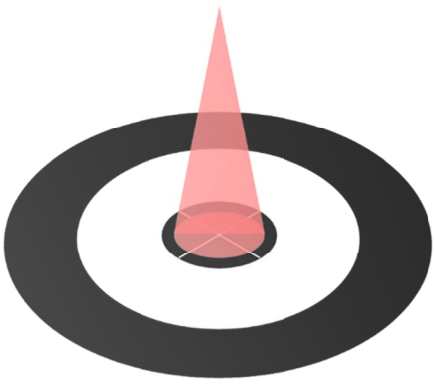

Fig. 6. An oversimplified schematic of a four quadrant detector annular dark field system for DPC analysis

Although Lorentz-TEM is useful for analysis of the distribution and mobility of the domain wall boundaries it is limited in terms of analysis of the magnetization vector spatial distribution and intensity. Hence, Lorentz-TEM analysis was complemented by LM-STEM DPC technique [8].

An oversimplified schematic illustration of the four quadrant annular dark field (ADF) detector system utilised for STEM-DPC imaging is given in the Fig. 6 [9]. On the figure it is sketched how a transmitted beam hits the detector and depending on the Lorentz force the quadrant towards the beam is deflected receives more signal relative to the opposing segment. The resulting microstructure can look like the example microstructures provided in the Fig. 7. The microstructures were recorded for the

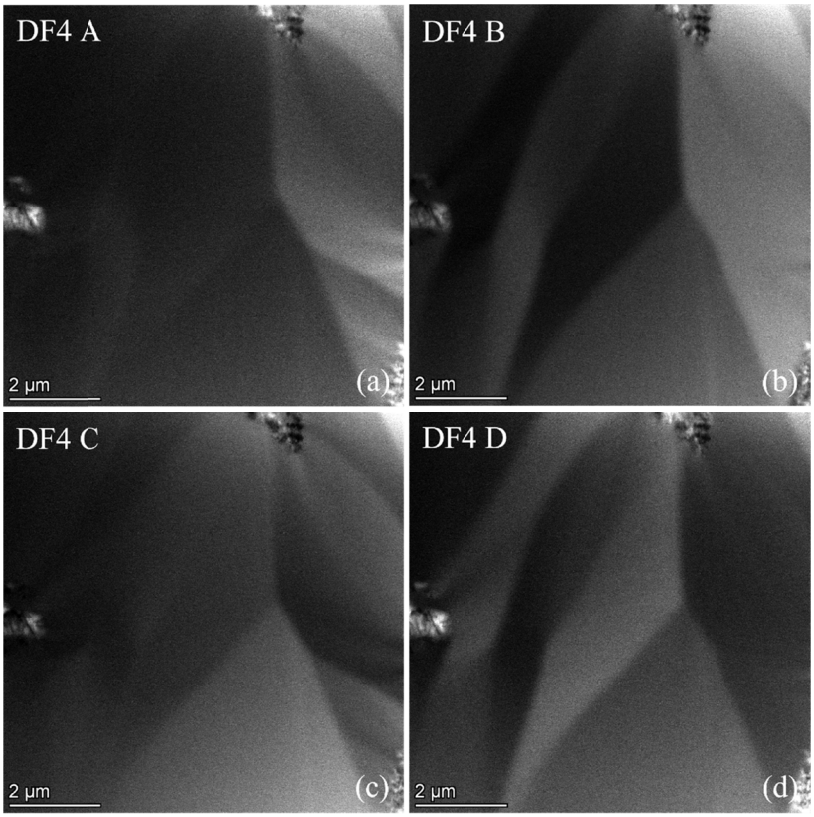

Fig. 7. STEM Dark Field (DF) images recorded with the four segment detector system

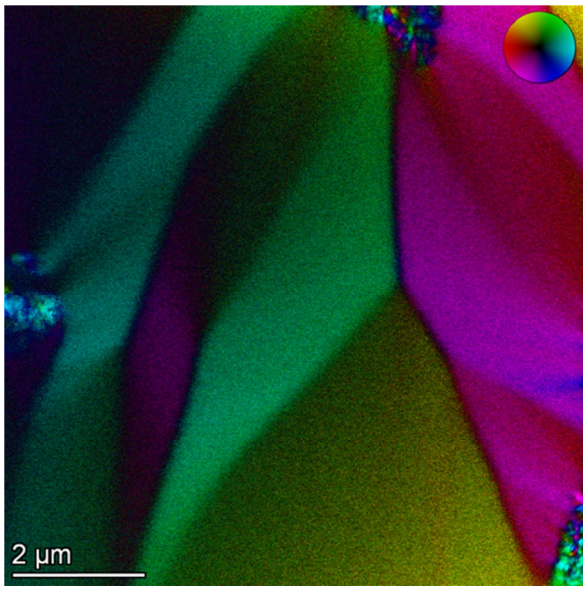

Fig. 8. LM-STEM DPC image of the selected area taken from the thin lamella of the $Fe_{69}B_{20}Nb_2Hf_2Si_2Y_5$ alloy

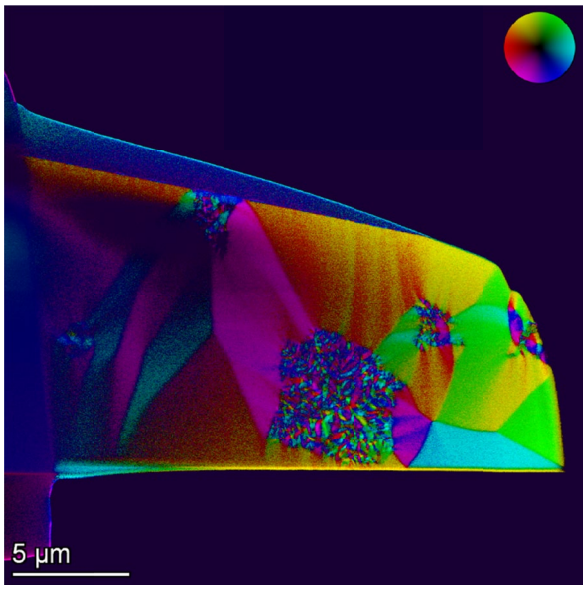

Fig. 9. LM-STEM DPC of the thin foil cut out from the $Fe_{69}B_{20}Nb_2Hf_2Si_2Y_5$ alloy

thin foil of the $Fe_{69}B_{20}Nb_2Hf_2Si_2Y_5$ alloy. One can note distinct contrast changes between the images (Fig. 7a-d). The resulting LM STEM DPC image, reconstructed based on the Fig. 7, is given in the Fig. 8. Colour wheel is included in the image for indication of the orientation distribution, whereas the colour intensity designates the intensity of the magnetic field. An overview LM-STEM DPC image of the whole lamella is given in the Fig. 9. The observed magnetic domain size, arrangement and distribution are in accordance with the Lorentz-TEM analysis (Fig. 2). It is noted that the dendritic structures also display colour coded contrast changes, which suggests they have internal submicron domain microstructure. The domains in their instance are confined in size by the grain boundaries.

Overall the thin lamella of the $Fe_{69}B_{20}Nb_2Hf_2Si_2Y_5$ alloy shows a complex magnetic domain microstructure well revealed by the Lorentz-TEM and LM-STEM DPC analysis.

4. Conclusions

The as suction cast alloy shows a complex magnetic macrostructure elucidated by Lorentz-TEM and LM-STEM DPC analysis. The magnetic domains are large and easily mobile, what indicates low coercivity. The domain wall movement is pinned to some extent by the presence of dendrites, that themselves show an internal submicrometric magnetic domain microstructure. The average domain wall width is estimated at 52 nm. The LM-STEM DPC results complement Lorentz-TEM analysis by providing more detailed insights on the magnetic vector distribution and its intensity within the domains. On the whole combined Lorentz-TEM and LM-STEM DPC become and indispensable tool for detailed studies of magnetic microstructures in soft ferromagnets.

Acknowledgements

The work was supported by the Institute of Metallurgy and Materials Science of the Polish Academy of Sciences within the statutory tasks: Z-14.

REFERENCES

[1] B.D. Cullity, C.D. Graham, Introduction to Magnetic Materials, IEEE PRESS, 2009.

[2] J.N. Chapman, The investigation of magnetic domain structures in thin foils by electron microscopy, J. Phys. D: Appl. Phys. **17**, 623-647 (1984).

[3] A. Ishizuka, K. Ishizuka, Observation of phase objects using STEM-Differential Phase Contrast (DPC) microscopy, JEOL News **55** 24-31 (2020).

[4] N. Shibata, S.D. Findlay, Y. Kohno, H. Sawada, Y. Kondo, Y. Ikuhara, Differential phase-contrast microscopy at atomic resolution, Nat. Phys. **8**, 611-615 (2012).

[5] G. Herzer, Modern soft magnets: amorphous and nanocrystalline materials, Acta Mat. **61**, 718-734 (2013).

[6] P. Czaja, M. Nabiałek, Evolution of microstructure and magnetic domains in $Fe_{74}B_{20}Nb_2Hf_2Si_2$ soft magnetic alloy studied by in-situ ultra-rapid heating TEM and Lorentz TEM microscopy, Acta Phys. Pol. A**142**, 17-20 (2022).

[7] T. Suzuki, A. Hubert, Determination of ferromagnetic domain wall widths by means of high voltage Lorentz microscopy, Phys. Stat. Sol. **38**, K5-K8 (1970).

[8] D.T. Ngo, L.T. Kuhn, In situ transmission electron microscopy for magnetic nanostructures, Adv. Nat. Sci.: Nanoscience and Nanotechnology **7**, 045001 (2016).

[9] N. Shibata, Atomic resolution differential phase contrast electron microscopy, J. Ceram. Soc. Jpn. **127**, 708-714 (2019).